

4.2 Hydrogeological investigations

4.2.1 Overview

4.2.1.1 Objectives

The objectives of the hydrogeological investigations are based on those set for the entire MIU Project and its individual Phases as follows ⁽⁷⁾.

Acquisition of the hydrogeological properties of those geological units, features, structures (faults, fractures, etc.) that could be flowpaths for groundwater and determination of the hydraulic heterogeneity of the rock mass due to lithofacies, weathering, alteration, etc.

Construction of hydrogeological model and testing or assessing its validity

Understanding the hydrogeology in the Shobasama Site and prediction of changes to the flow system (drawdown) and of the amount of water inflow into the shafts caused by shaft excavation

Development of methodologies for systematic investigations and analyses of hydrogeology

4.2.1.2 Performance and development of the study

It is important to ascertain the following:

- Thorough understanding of the information obtained,
- Understand the uncertainty in data and models,
- Priority of data acquisition for decreasing uncertainty

The study is expected to evaluate and decrease uncertainty by performing an “analysis loop of groundwater hydrology” (Figures 3.1 and 4.25).

4.2.1.3 Development of the conceptual hydrogeological model

In the geological investigations a number of geological models were developed at the regional scale for the about 4 km × about 6 km study area and at the detailed scale for the Shobasama Site (0.8 km × 1.3 km). At both scales the distributions of the geological units were outlined in 3-D space. These conceptual geological models provide the framework for the hydrogeological models investigated.

Hydrogeological models in the rock mass are classified into a continuum model that treats the rock mass as a porous continuous medium and a fracture network model that takes structural discontinuities such as fractures into consideration. In the MIU Project, both porous continuum and fracture network models are to be adopted to examine the applicability of each modeling methodology.

In Phase I-a (1996-1999), the continuum model was adopted for the following reasons:

- Information on the distribution of fractures and their hydrogeological properties were not available in sufficient detail to develop a discrete fracture model
- Time and computation constraints

4.2.1.4 Phase I-a hydrogeological investigations and analyses

During Phase I-a, two analysis loops were implemented. In the 1st analysis loop, only the hydrogeological information obtained from the about 4 km × about 6 km study area and the studies in the Tono Mine were used for construction of the hydrogeological model and performance of the groundwater flow simulation.

In the 2nd analysis loop, the information obtained in Phase I-a of the MIU Project was combined with the data used in the 1st analysis loop to improve the hydrogeological model and groundwater flow simulation. In the 2nd analysis loop, problems identified during the 1st analysis loop were taken into consideration.

4.2.2 Hydrogeological model and groundwater flow simulation (1st analysis loop)

4.2.2.1 Overview

The hydrogeological model used in the 1st analysis loop is constructed from the conceptual geological model for the regional study area, about 4 km × about 6 km encompassing the Shobasama Site.

The purposes of construction of the hydrogeological model and groundwater flow simulations in the 1st analysis loop are as follows:

- Develop an understanding of the general hydrology and hydrogeology in and around the Shobasama Site
- Begin to develop the expertise and methodology needed in future to predict impact on hydrogeology caused by shaft excavations
- Identify problems to be solved in the subsequent investigations and analyses

The study area

The study area (about 4 km × about 6 km, Figure 4.26) encompasses the Shobasama Site. It is surrounded by ridges and streams that are considered to be groundwater flow boundaries. It was selected because it is regional in scale and considered to include a complete regional flow system from recharge to discharge. The results of the RHS Project ⁽⁴⁶⁾ indicate that mountain ridges generally form hydraulic boundaries. Selecting an area this size is intended to improve the accuracy of groundwater flow simulation.. The depth of this study area is set as GL-3,000 m. This takes the depth of planned shafts for the MIU Project and the scale of the study area into consideration.

Schedule of shaft excavation (developed pre-1998)

For the flow simulation, the planned shaft for the MIU Project is included. The parameters are outlined below.

The planned depth and diameter are 1,000 m and 6 m, respectively. Based on preliminary designs before 1998 FY, it was planned to do the excavation in the following stages (Figure 4.27).

- Excavation from ground surface to 500 m depth
- 6 month investigation stage
- Excavation from 500 m to 900 m depth
- Three-year investigation stage
- Excavation from 900 m to 1,000 m depth

The shaft is included in the simulation because it is expected to have the strongest hydraulic impact (sink) on the flow system and on storage in the surrounding rock mass.

Development of the numerical model for the groundwater flow simulation

A finite element method (FEM)-based on the 3-D saturated/unsaturated seepage flow simulation program (TAGSAC) ⁽⁴⁷⁾ was adopted. TAGSAC was developed for modeling porous media. A steady-state simulation taking the Tono Mine into consideration and a transient simulation for predicting the groundwater hydrology affected by the shaft excavation were carried out.

4.2.2.2 Construction of the hydrogeological model

The 3-D simulation mesh

The about 4 km × about 6 km study area was modeled by generating a 3-D simulation mesh to carry out the FEM-based 3-D saturated/unsaturated seepage flow simulation. The procedures are as follows.

The surface of the 24 km² study area was divided into a grid on a 2-D plane so that the Tsukiyoshi Fault, the boreholes, the planned shafts for the MIU Project and the Tono Mine shafts were represented. The number of element divisions are 875 (25 EW × 35 NS). Elevations of the individual nodes are calculated from the 20 m-interval digital elevation data to express the topography of the study area (Figure 4.28). The ground surface elevation ranges from 134 to 380 masl.

The 3-D mesh (FEM model) was prepared by dividing the rock mass from surface to the bottom of the study area into 20 horizontal layers. The bottom of the model was set at -3,000 masl. Also included in the 3-D mesh are the shafts and galleries of the Tono Mine. For the Tsukiyoshi Fault, 1 m-wide platy elements are set stepwise to make the element division easy. The number of nodal points and elements in the 3-D simulation mesh measures 19,656 and 17,500, respectively. The hydrogeological model is shown in Figure 4.29.

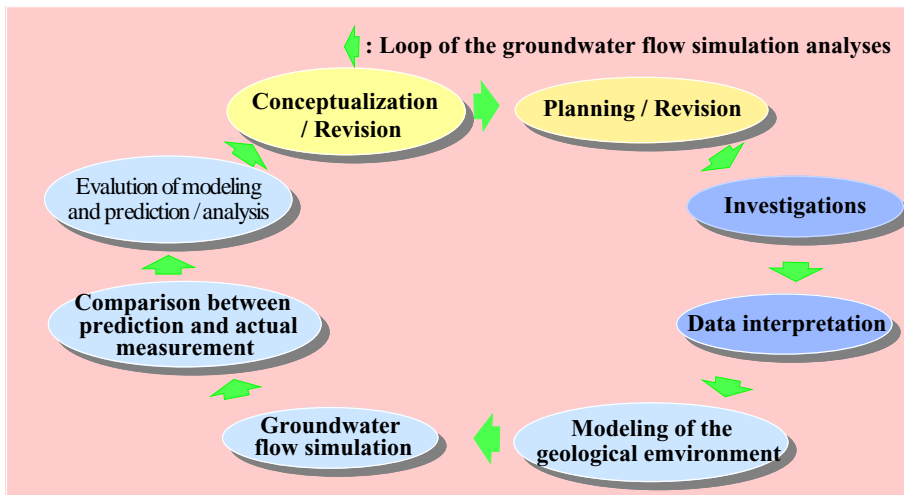


Figure 4.25 Approach to investigations, analysis, modeling and flow simulation

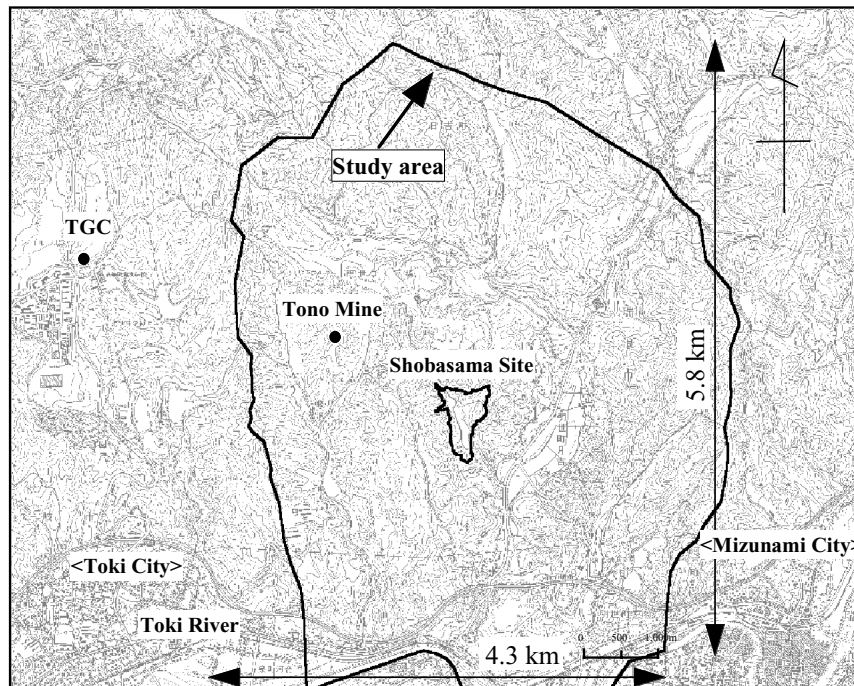


Figure 4.26 Location map of study area and Shobasama Site

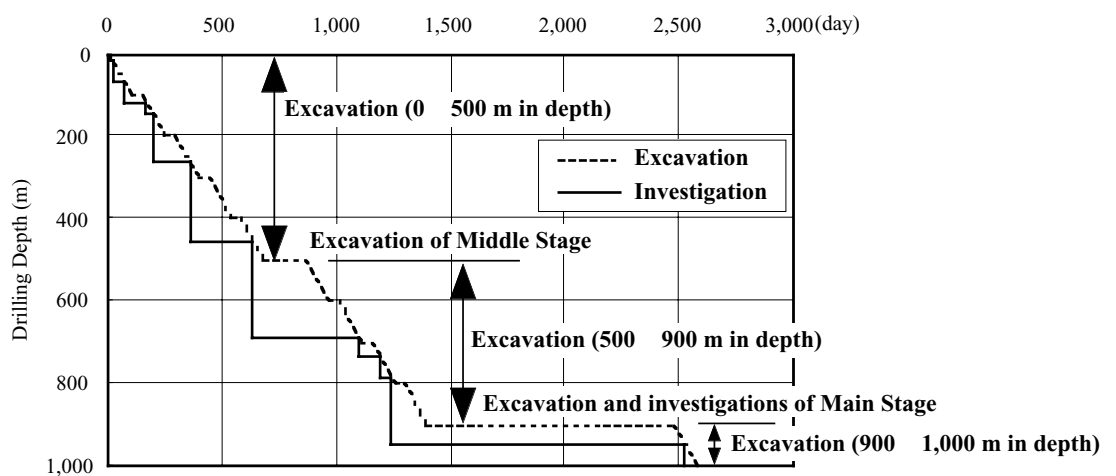


Figure 4.27 Schedule of shaft excavation and investigations as of 1998 FY

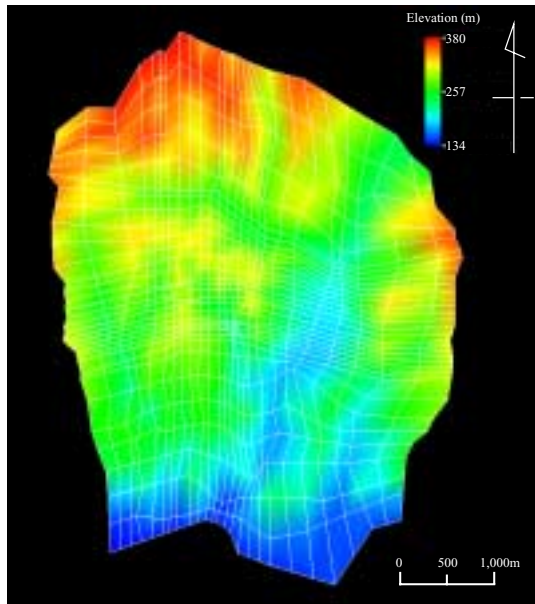


Figure 4.28 Finite element mesh and altitude distribution of model top boundary

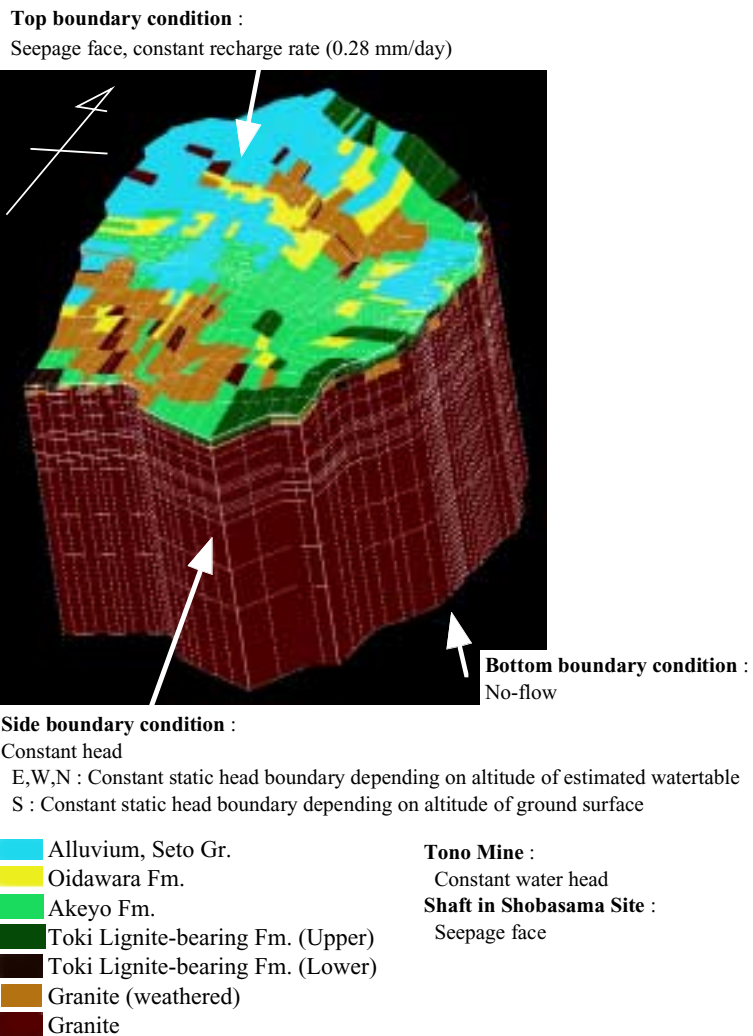


Figure 4.29 Hydrogeological model

Stratigraphy, lithology and hydrogeological properties

The 3-D simulation mesh was fit to the geological model (about 4 km × about 6 km : Section 4.1.4). However, the mesh layers do not always directly corresponds with the thickness of the individual geological units of the geological model. Therefore, any geological units at the center of the mesh are allocated to the 3-D simulation mesh. The hydraulic conductivity values in Table 4.13 are established for each geological unit on the assumption that each geological formation is hydrogeologically homogeneous and behaves as a continuum. These values are based on data from the RHZ and the results ⁽⁴⁸⁾ of groundwater flow simulations in and around the Tono Mine. Permeability in unsaturated domains was set based on the moisture characteristic curve and relative hydraulic conductivity curve shown in Figure 4.30 (49 ~ 51).

Table 4.13 Hydraulic conductivities of the geological units

Geology	Hydraulic conductivity (m/s)
Seto Group	1.0×10^{-7}
Oidawara Fm.	1.0×10^{-9}
Akeyo Fm.	1.0×10^{-9}
Toki Lignite-bearing Fm. (Upper)	5.0×10^{-9}
Toki Lignite-bearing Fm. (Lower)	1.0×10^{-8}
Toki granite (Weathered)	1.0×10^{-7}
“Moderately fractured zone”	1.0×10^{-9}
Tsukiyoshi Fault	1.0×10^{-10}

Establishing boundary conditions

Top boundary condition

The top boundary was based on digitization of the topographic map of the Tono area. Recharge at the top boundary takes precipitation, evaporation and run-off into consideration. The recharge rate of 0.28mm/day, ⁽⁵²⁾ an average rate calculated from observations between 1990 and 1997 in the vicinity of the Tono Mine, was adopted on the assumption that the recharge rate in the larger study area is the same. The ground surface is set as a free seepage face.

Bottom boundary condition

The bottom boundary, at -3,000 masl was set as a no-flow boundary.

Side boundary conditions

The side, groundwater flow boundaries coincide with mountain ridges (the northern, eastern and western boundaries) and the Toki River (the southern boundary). The ridges could be considered as watershed divides; however, some studies point out that these ridges are not always coincident with watershed boundaries because of local geological structures. In addition, the results ⁽⁵³⁾ of groundwater flow simulations for the larger RHS, encompassing the study area, indicates southwestward groundwater flow controlled by regional topography. Accordingly, side boundaries along the ridges are set as permeable, and constant head. The constant heads assigned to the boundaries are determined by the following equation, which formulates the relationship between surface elevations and the water levels observed in boreholes around the study area (Figure 4.31).

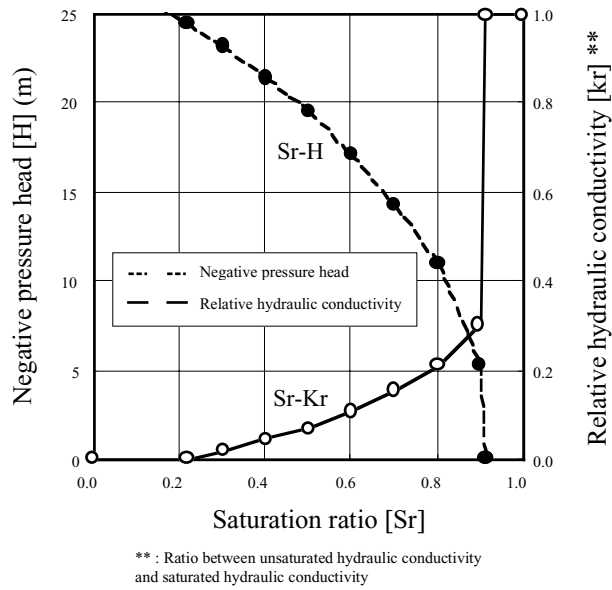
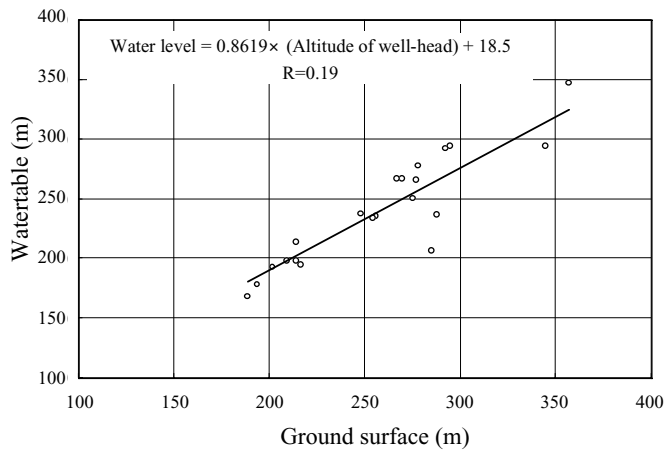


Figure 4.30 Moisture characteristic curve and relative hydraulic conductivity curve



n=21

AN-1	DH-1 ⁵⁴⁾	KA-3
AN-3	DH-2 ⁵⁵⁾	SN-1
AN-4	DH-3 ⁵⁶⁾	SN-2
AN-5	DH-4	SN-3
AN-6	HN-1	SN-4
AN-7	KA-1	SN-5
AN-8	KA-2	SN-6

(Data obtained from these boreholes)

Figure 4.31 Relationship between elevation of ground surface and watertable

$$(\text{Constant head (masl)}) = 0.86 \times H (\text{elevation of each location in masl}) + 18.5$$

The boundary along the Toki River is also set as permeable, and constant static head. Surface elevation is used as the constant head assigned to the boundary.

Tono Mine and planned shaft for the MIU Project

The galleries in the Tono Mine are assigned a pressure head of 0 m, because the galleries are at atmospheric pressure.

As for the planned shaft in the MIU Project, the geological units are removed from the hydrogeological model one by one in response to the progress of shaft excavation. Nodal points representing the shaft wall are set as free seepage points on the assumption that all the groundwater seeping into the shaft will be pumped to surface.

4.2.2.3 Groundwater flow simulation

Steady-state simulation (simulation of undisturbed groundwater conditions)

Prior to a transient simulation (simulation of the disturbance due to shaft excavation), a steady simulation was carried out. The simulation was intended to develop an understanding of the groundwater hydrogeology but takes the existence of the Tono Mine in the study area into consideration. The validity of the simulation is tested by comparing the simulated results with the head distributions in boreholes in the study area.

Comparison of simulated results with head distribution data

Figure 4.32 shows the comparisons between distributions of the measured hydraulic heads and the simulated results.

The simulation model described above employs coarser meshes than the model used for the groundwater flow simulation carried out around the Tono Mine⁽⁴⁸⁾ and gives insufficient consideration to the position of the Tsukiyoshi Fault. Nonetheless, the distributions of groundwater pressure measured in AN-1, 6, 7 and 8, drilled largely in sedimentary rocks around the Tono Mine, are closely matched by the model's simulation of drop in head due to the existence of the Mine. Also, the general trend of head distributions is reproduced well (Figure 4.32 (a), (b), (c) and (d)).

Simulated values for DH-9, drilled largely in granite, (Figure 4.32 (e)) are also coincident with the measured values of trend of head. However, the simulated values are higher than the measured values. This discrepancy of about 30 m is thought to be caused by inaccuracies in the hydrogeological model, as follows:

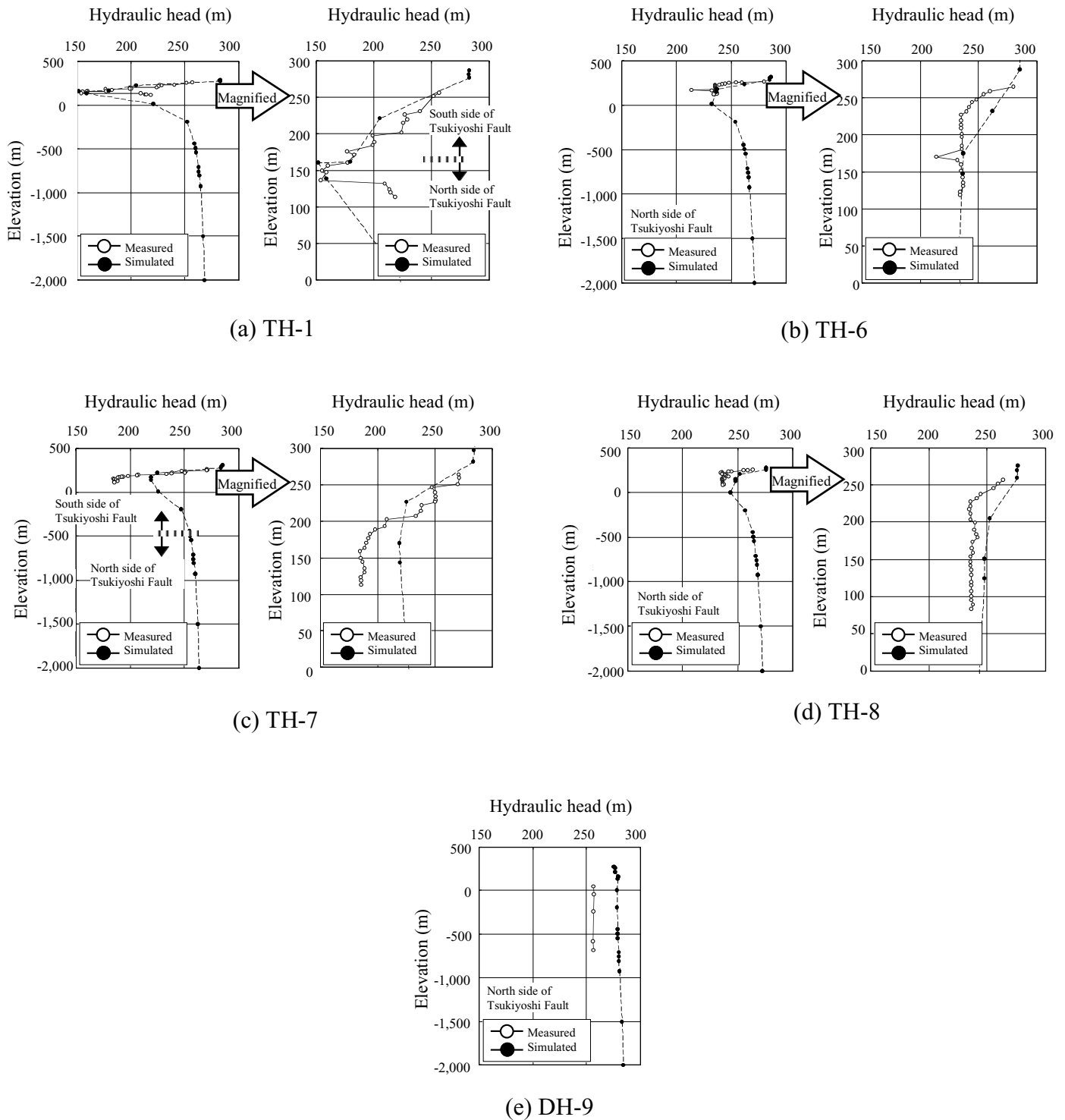


Figure 4.32 Head distribution (comparison between measured data and simulated data)

- Permeability contrast generated by the Tsukiyoshi Fault
- Top boundary condition; i.e., recharge rate
- Position/shape of the Tsukiyoshi Fault

Groundwater hydrogeology in the undisturbed state

This steady-state simulation shows the following results on the distribution of heads and Darcy velocity vectors (Figure 4.33). Figure 4.34 shows the cross sections of the simulated results.

Heads in the study area generally decrease from north to south (Figure 4.33 (1, 2 and 3)) indicating that the groundwater flows generally from north to south as a whole.

The flow of groundwater above an elevation of 0 masl (“shallower part”) is more affected by the topography of the ground surface than is the flow below an elevation of -758masl (“deeper part”). As a result, local variations in head and Darcy velocity vector distributions are generated (a, c in Figure 4.33 (1); d in Figure 4.33 (3); e in Figure 4.33 (4)). The shallower part, being more permeable and sensitive to the top boundary condition than the deeper part, gives rise to larger values of Darcy velocity vectors (Figures 4.33 (3) and (4)). The distribution of Darcy velocity vectors is locally disturbed around the Tono Mine (b in Figure 4.33 (1)).

The head distributions in the deeper part gently varies. The Darcy velocity vectors are nearly horizontal from north to south (Figure 4.33 (3)) suggesting that the deeper part is hardly affected by the topography of the ground surface and the local flow systems developed.

The groundwater flow simulation based on the current hydrogeological model indicates that the Tsukiyoshi Fault exerts only a small influence on the distribution of heads and Darcy velocity vectors (Figure 4.33 (1), (2), (3) and (4)).

Transient simulation (predictive simulation of disturbance to groundwater flow due to MIU shaft excavation)

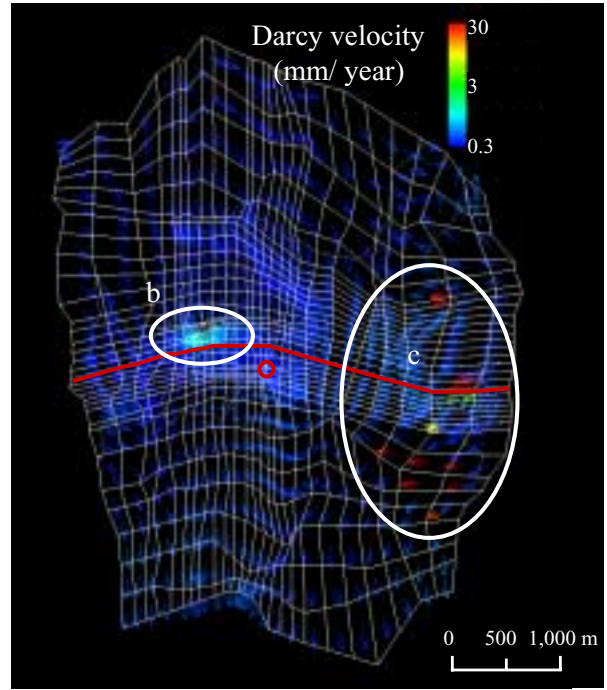
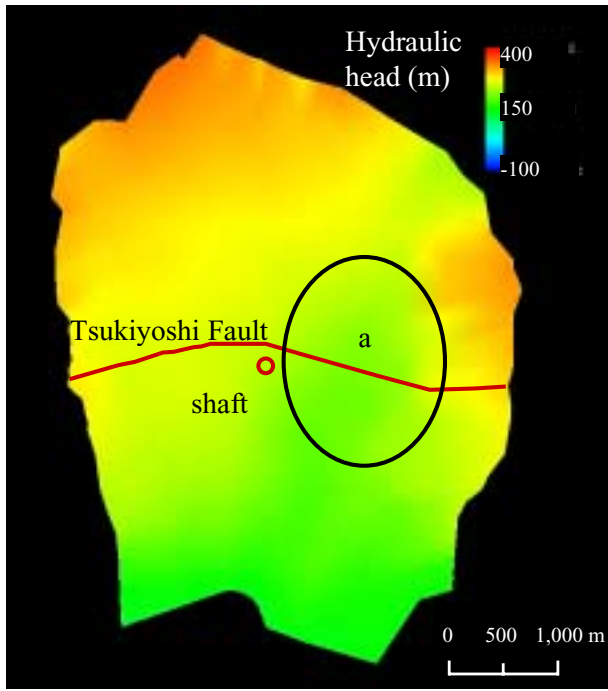
The transient simulation was carried out on the assumption that MIU shaft would be excavated on the schedule as shown in Figure 4.27.

Simulation results: effect on heads and Darcy velocities

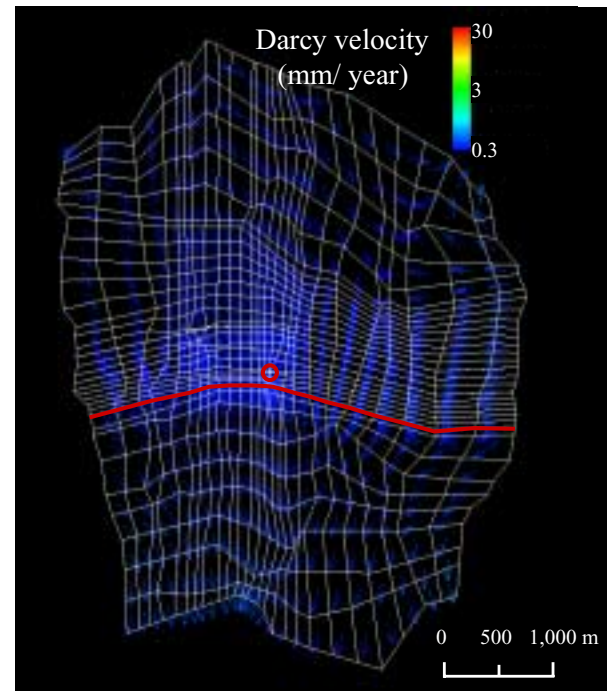
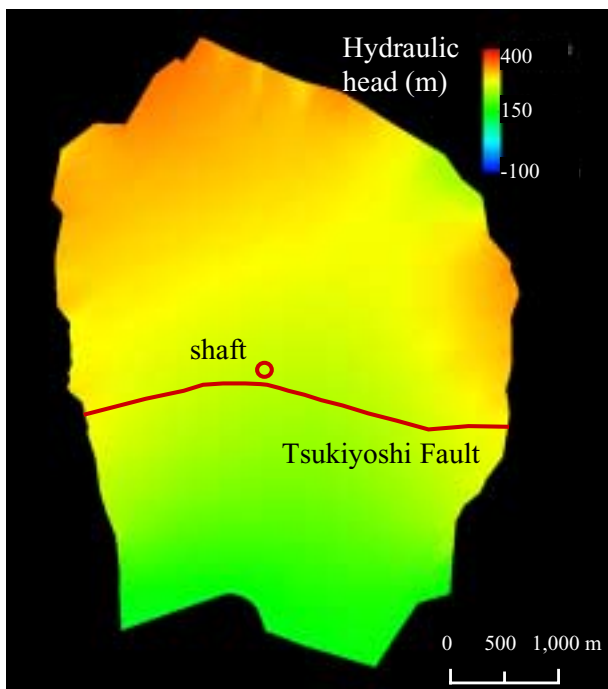
The results of predictive simulation of groundwater hydrogeology caused by shaft excavation are summarized below and shown in Figure 4.35. The cross sections shown in Figure 4.35 are along the same planes as those in Figure 4.34.

Heads are lowered around the shaft. The groundwater around the shaft not only flows but also changes the potential or gradient toward the shaft with the result that Darcy velocities toward the shaft increase.

The groundwater flows upward, into the shaft at depths greater than 1,000 m in the region of the shaft, (Figure 4.35 (2), (3)).

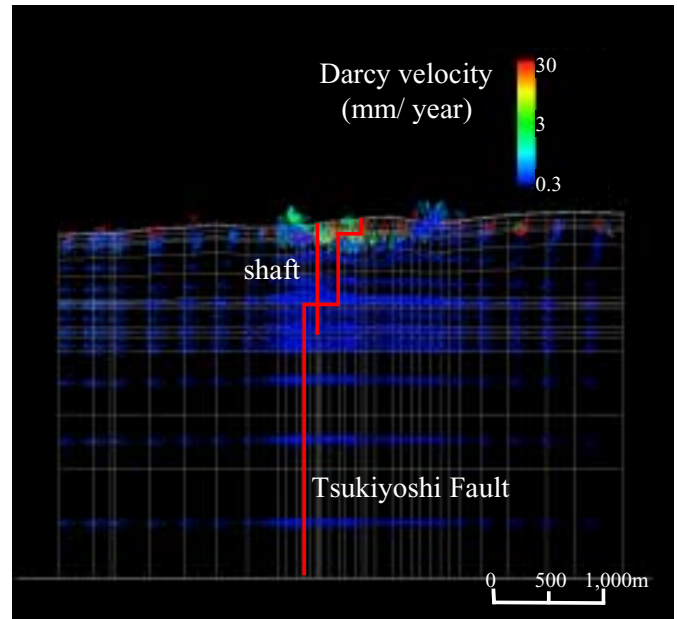
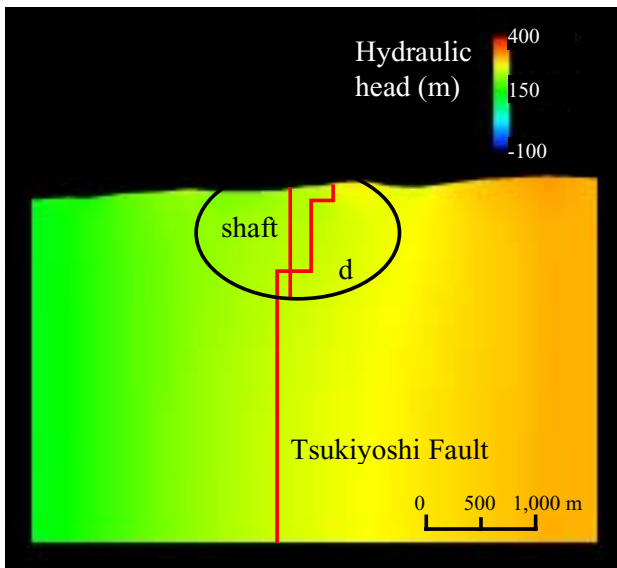


(1) Head and Darcy velocity vector in the horizontal plane at the altitude of 0 m

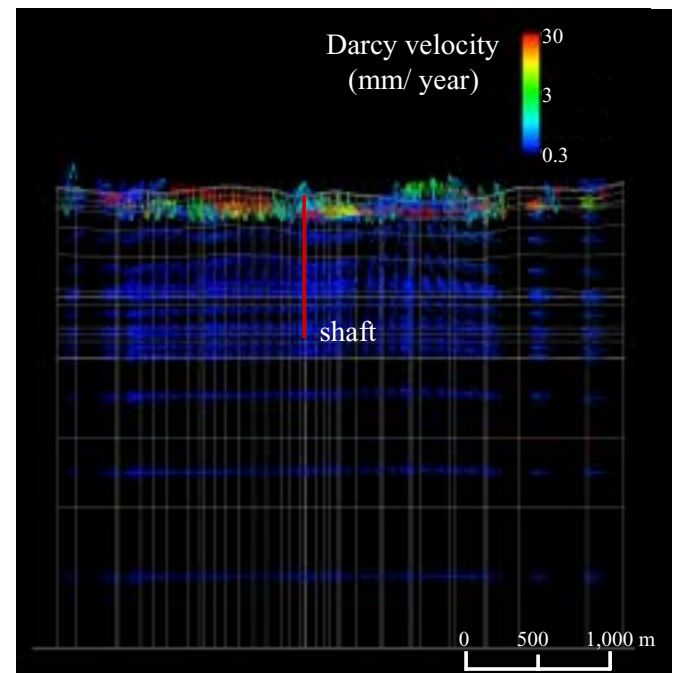
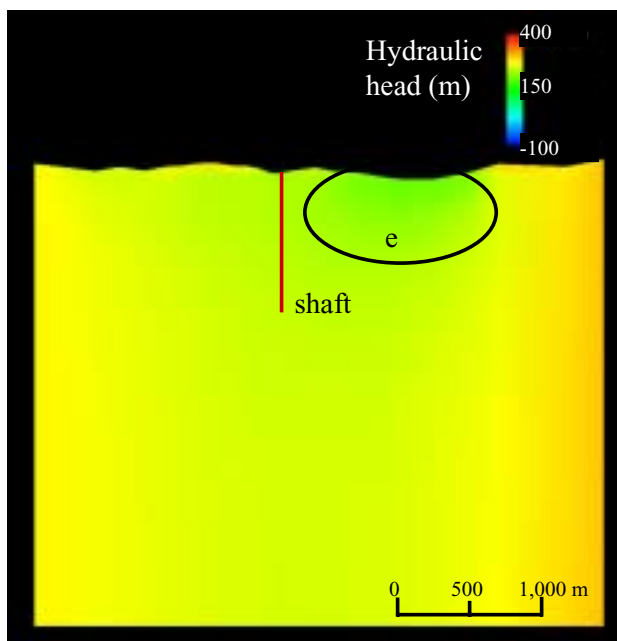


(2) Head and Darcy velocity vector in the horizontal plane at the altitude of -758 m

Figure 4.33 The result of groundwater flow simulation (Steady state) (1/2)

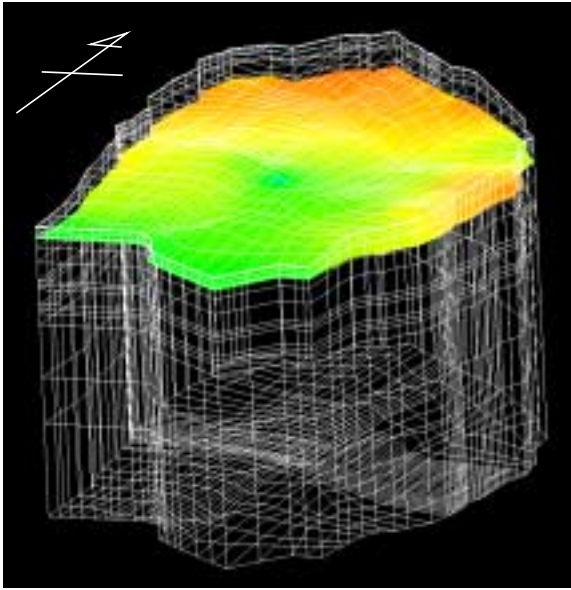


(3) Head and Darcy velocity vector in N-S section passing through the shaft

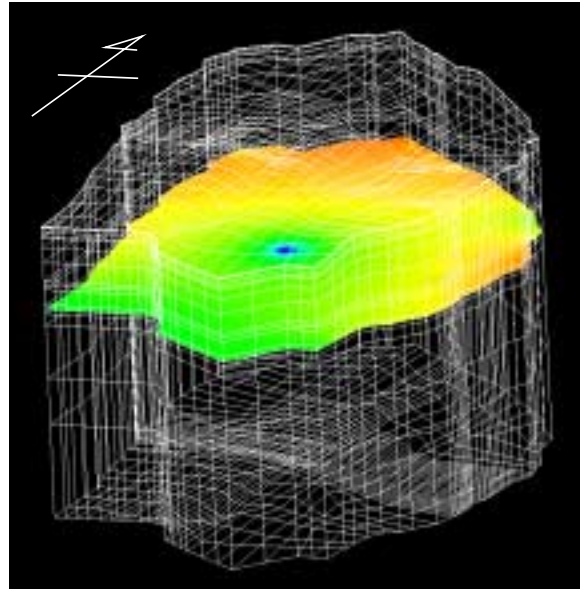


(4) Head and Darcy velocity vector in E-W section passing through the shaft

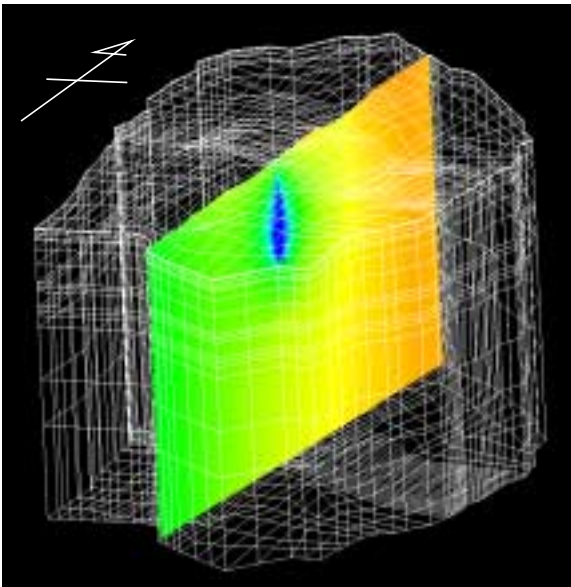
Figure 4.33 The result of groundwater flow simulation (Steady state) (2/2)



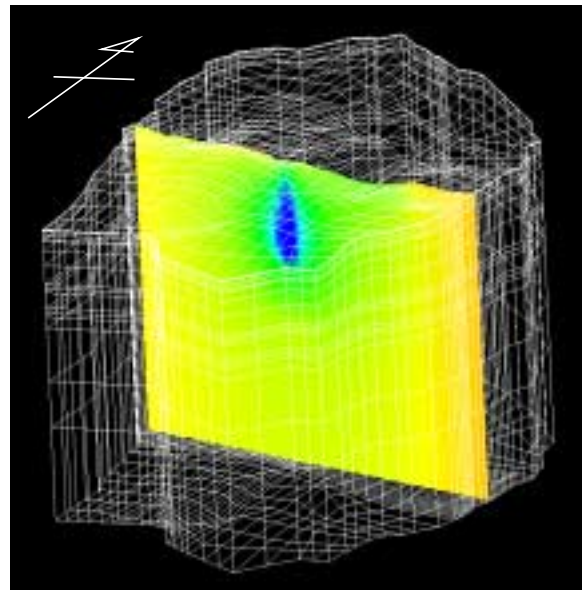
(a) Section 1 : Horizontal plane at the altitude of 0 masl



(b) Section 2 : Horizontal plane at the altitude of -758 masl

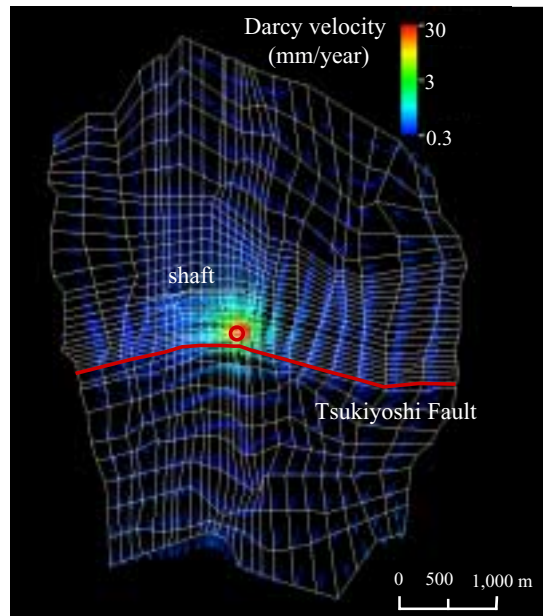
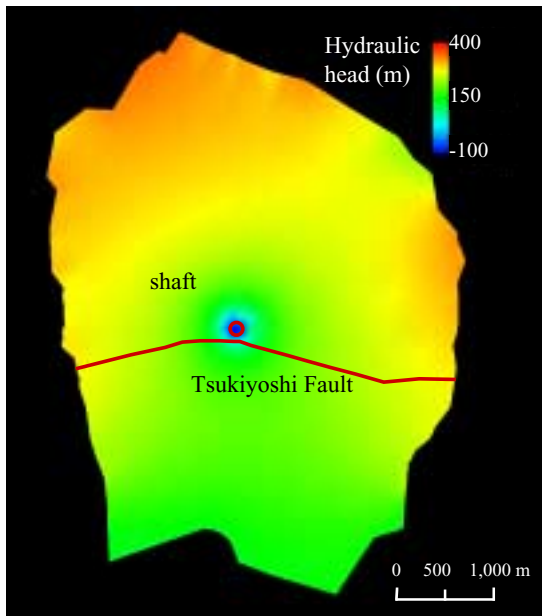


(c) Section 3 : N-S Section passing through the shaft

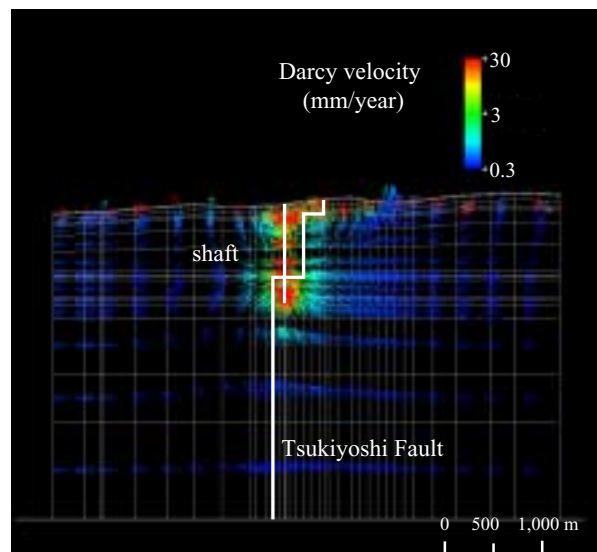
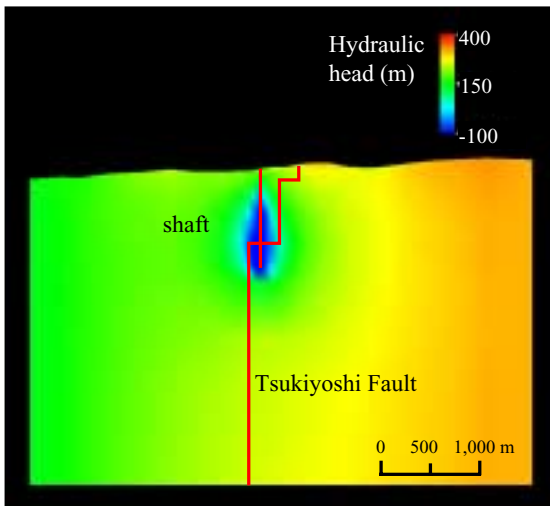


(d) Section 4 : E-W section passing through the shaft

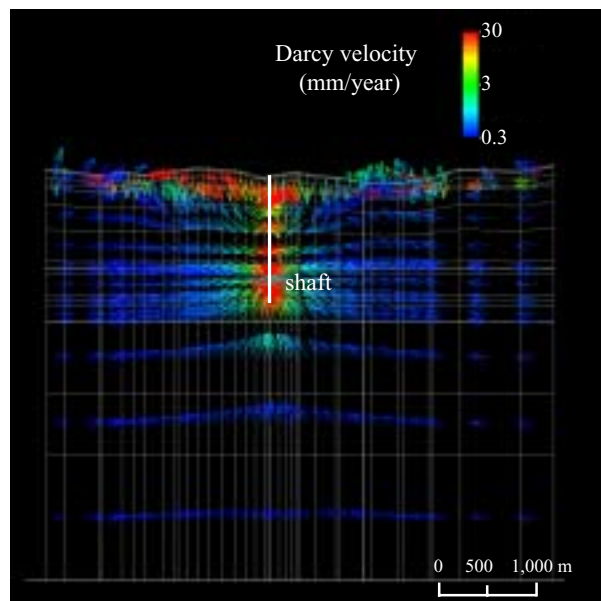
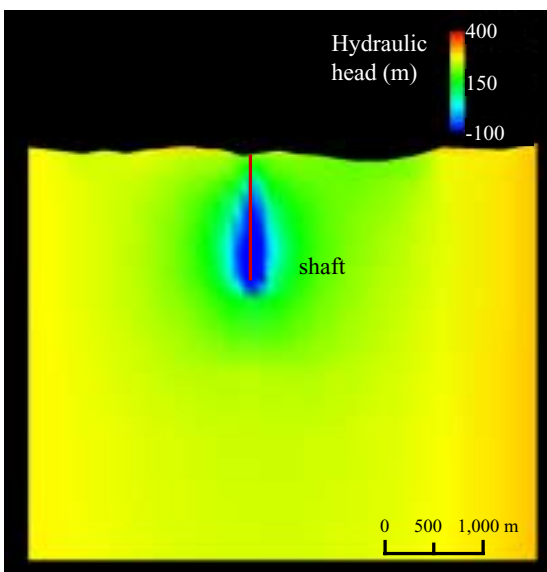
Figure 4.34 The result of groundwater flow simulation (cross section)



(1) Hydraulic head and Darcy velocity vector at the altitude of -758 m



(2) Hydraulic and Darcy velocity vector in N-S section passing through the shaft



(3) Hydraulic and Darcy velocity vector in E-W section passing through the shaft

Figure 4.35 The results of the predictive simulation

Simulation results: effect on groundwater hydrogeology

Changes in groundwater hydrogeology caused by MIU shaft excavation are as follows (Figure 4.36). The cross sections in Figure 4.36 are along the same planes as in Figure 4.34.

The drawdown on the horizontal plane at surface shows a nearly concentric pattern of drop in head with the shaft as the center. This indicates that the Tsukiyoshi Fault exerts negligible influence on the groundwater flow in the simulation with the properties currently included in the hydrogeological model.

The distribution of drawdown in vertical N-S and E-W sections that include the shaft shows an onion-shaped pattern (Figure 4.36 (1), (2)). This suggests that properties assigned to the upper geological units are such that the heads near the surface are prevented from falling.

Drawdown effects due to shaft excavation are within the boundaries of the about 4 km × about 6 km study area (Figure 4.36).

4.2.2.4 Evaluation of boundary conditions

Evaluation of the results of the 1st analysis loop has identified the following problems to be solved during the 2nd analysis loop.

For the steady-state-simulation, the results approximately reproduce the existing groundwater hydrogeology. It suggests that the boundaries as defined are appropriate. However, simulated values are generally a little larger than measured values. This can be caused by the method of establishing the relationship between groundwater level and elevation, on which the hydrostatic pressure assigned to the side boundaries are based (Figure 4.29). It is also possible that overestimation of the recharge rate is the cause. Thus, these should be considered in the 2nd analysis loop.

The transient simulation results show a small drawdown in shallow part of the model, despite the shaft excavation as shown in Figure 4.36. It suggests that perhaps the recharge rate exerts a greater effect on groundwater hydrology in the shallow part than considered previously. Therefore, it may be necessary to assign recharge rates according to the properties of individual areas and the underlying geological formations instead of giving an averaged value to the study area.

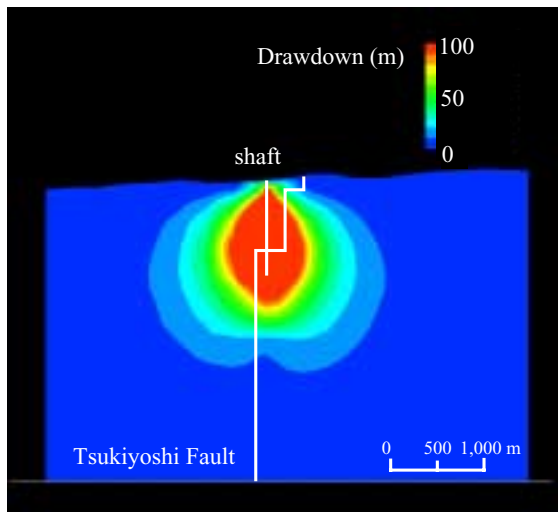
Effects of the shaft excavation do not extend to the bottom boundary of the study area. This suggests that it is appropriate to define the bottom boundary to be a no-flow boundary at the depth used in this simulation.

4.2.2.5 Summary

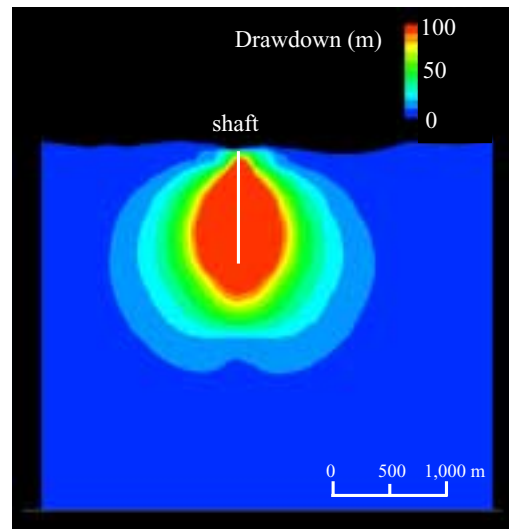
Simulation results are as follows.

The groundwater flows from north to south.

Drawdowns caused by the shaft excavation are within the boundaries of the about 4 km × about 6 km model area. It suggests that the size of the study area is appropriate for understanding the extent of area affected by the shaft excavation.



(1) Drawdown in N-S section passing through the shaft



(2) Drawdown in E-W section passing through the shaft

Figure 4.36 Distribution of drawdown immediately after the completion of shaft excavation

In the groundwater flow simulation using the hydrogeological model, the horizontal distribution of the drawdown shows a concentric pattern with the shaft as its center. It does not indicate that the Tsukiyoshi Fault forms an impervious zone.

The simulation results shows the size of the study area and setting of the boundary conditions used for this simulation could be used for 2nd analysis loop.

4.2.2.6 Future tasks

While the steady-state and transient flow simulations allow understanding the overall groundwater hydrogeology in the study area, none of the investigation results obtained in the area were used for these simulations. The following are extracted as tasks to be dealt with in the future.

Examine the method of establishing the geological units for the geological model; especially taking the heterogeneity of granite into consideration

Consider the variety, quantity and quality of information (the data requirements) needed for modeling and groundwater flow simulation

Understanding the hydrogeological properties of individual geological units and predict the 3-D distribution of hydraulic conductivity

Methodology for construction of the hydrogeological model

Consider the method for estimating 3-D distribution of hydraulic conductivity

Methodology of groundwater flow simulation

Consider the methods for saturated/unsaturated simulations and the applicability of finite element and finite difference methods.

Method of setting hydraulic boundary conditions

Consider the method and basis for the top and side boundary conditions, considering the available data

Assessment of the uncertainty inherent in data obtained, in models and in the groundwater flow simulation

Consider which factors could contribute to reduction of the uncertainty, and, if possible, the prioritization of data acquisition.

4.2.3 Hydrogeological model and groundwater flow simulation (2nd analysis loop)

4.2.3.1 Overview

The groundwater flow simulations carried out for the 2nd analysis loop are based on enhancements to the geological models with data and knowledge from additional hydrological data, borehole investigations in three 1,000 m-deep boreholes (MIU-1, 2 and 3), reflection seismic surveys, and other data to be described below. The borehole investigations consisted of the following:

- Core descriptions and BTV investigations to acquire detailed information on location, orientation and style of fracture zones that are considered to be potential water conducting features (WCF) in the granite